IOP Conf. Series: Materials Science and Engineering **234** (2017) 012011 doi:10.1088/1757-899X/234/1/012011

Research on Aeroheating of Hypersonic Reentry Vehicle Base Flow Fields

Qin Xuguo[1], Shui Yongtao[1], Wang Yonghai[1], Chen Gang[1] and Li Qiang[1]

[1] Beijing Institute of Space Long March Vehicle; Beijing, China

by0405118@163.com

Abstract. The structure of the base flow of a hypersonic reentry vehicle and the resulting base pressure and heat transfer have been studied by numerical study. The compressible Navier-Stokes equations are solved by the finite-volume method. SST k-ω turbulence model is used, and comparisons are made with flight test. Attention was focused on assessing the effects of angle of attack and Mach number. It was found that angle of attack can significantly alter the wake flow structure and reentry vehicle base pressure and heating distributions. The results of the simulation may provide a theoretical basis for the design of the thermal protection system of hypersonic reentry vehicles.

1. Introduction

When the hypersonic flight vehicle reentr into the atmosphere, the problem of aerodynamic thermal protection has always been a problem to be considered in the hypersonic flight vehicle design. The high enthalpy flow field generated by hypersonic velocity will produce an extreme thermal environment. Thus, a thermal protection system must be designed.

The thermal environment at the bottom of the flight vehicle is lower than that of the tip and the large area. However, the material,size and weight of the bottom thermal protection system have a direct impact on the overall design, so the aerodynamic heating caused by the bottom flow has always been a hot topic. The prediction of the bottom thermal environment will directly affect the design of the hypersonic flight vehicle.

When the hypersonic flight vehicle reentry into the atmosphere, the bottom flow is very complex, including the mutual interference of shock wave, shear layer, recirculation zone, separation wake vortex and so on[1,2]. In the presence of an angle of attack, the structure of the wake flow field is tilted and the viscous shearing effect is enhanced, making the heat flow and pressure distribution different from the zero angle of attack. Most of the previous studies focused on the zero angle of attack[3-5], while few studies were about the angle of attack. When the experiment studies the bottom flow, its flow field is easy to be interfered and difficult to accurately measure owing to the impact of such support. Therefore, we can use wind tunnel experiment or flight test method to get the experimental data, conducting the CFD verification and then calculating the state that the experimental method cannot reach by adopting the CFD method.

In this paper, CFD method is used to simulate the distribution of bottom heat flow and pressure upon the reentry of hypersonic flight vehicle. The influence of the angle of attack and Ma number on the heat flow and pressure distribution is studied. The flow mechanism is also discussed. It provides supplementary reference for the wind tunnel experiment and the flight test of bottom heat flow.

2. Numerical Method

The simulation model is a simple cone. The length is L=3960mm. The radius of nose is 2.54mm, Ma_∞ =5,15,10,20,α=0°,5°,10°,15°,20°,25°,30°;P_∞=2801.55Pa,T_∞=221K. The altitude is H=24.38Km. The temperature of wall at base is T_{wb}=354K.

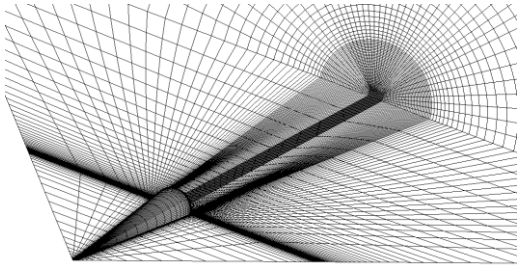

Figure 1. Three-dimensional grid for simulation.

Half model is used to be simulated, as shown in Figure 1. The vertex of nose is the origin of coordinates. The thickness of first layer of grid is 10^5 m. The overall three-dimensional multi-block grid consists of 1.6×10^5 points. The compressible Navier-Stokes equations are solved by the finite-volume method. SST k-ω turbulence model is used. Higher order Roe scheme is used, and the time term is solved by implicit scheme.

3. Computed result and analysis

3.1. Validation

The bottom flow of the hypersonic flight vehicle is complicated, which brings a lot of difficulties to the numerical simulation, so it is necessary to verify the numerical method. First, the flow field at Ma = 20, α = 0 ° is simulated and compared with the flight test results. As shown in Figure 2, the flight test values are more evenly distributed along the radial direction and the calculated heat flow peak value is bigger than the test value. The experimental results are in agreement with the results obtained in the literature [4] with DES method and literature [6] with RANS.

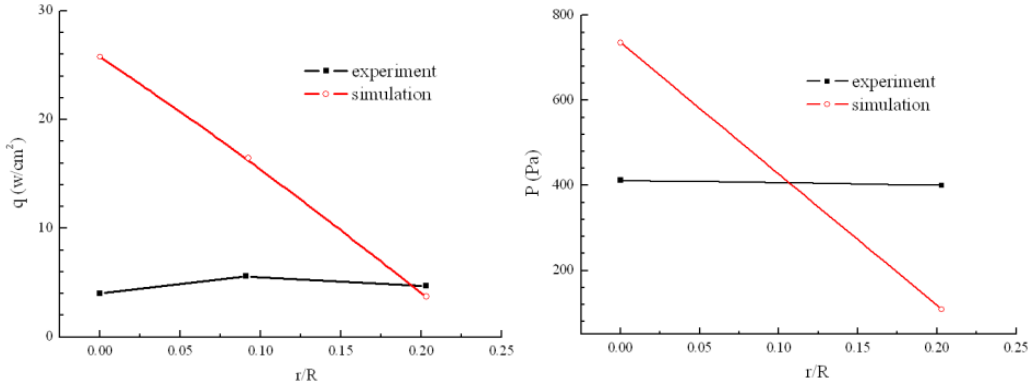

(a) Heat flux distribution (b) Pressure distribution

Figure 2. Comparison of calculated value and trial value.

3.2. Heat flux and pressure distribution with the effect of angle of attack

The effects of the angle of attack and Ma number on bottom heat flow and pressure are numerically simulated. The heat flow distribution on the bottom center line from the windward to the symmetry plane of the leeward side is shown in Figure 3. It can be seen that, at α= 0 ° , the heat flow peak value appears at the bottom of the center position. With the increase of the angle of attack, the heat flow

peak value moves toward the leeward side. The greater the Ma number, the more obvious the peak value of bottom heat flow that changes with the angle of attack.

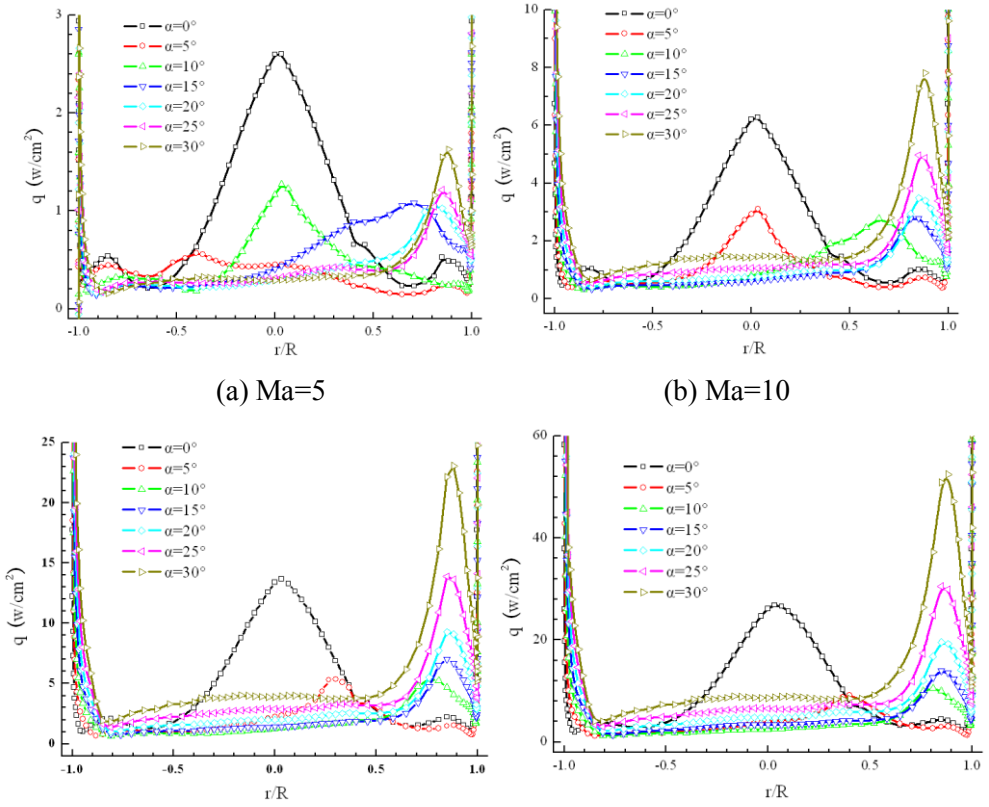

(a) Ma=5 (b) Ma=10

(c) Ma=15 (d) Ma=20

Figure 3. Heat flux of center line with the effect of angle of attack.

With the increase of the angle of attack, the peak value of the bottom heat flow decreases first and then increases. The minimum peak value of the bottom heat flow appears at the angle of attack α = 5 °. The peak value of bottom heat flow is smaller than that at α = 0 ° when the angle of attack increases to α = 30 ° for the smaller Ma number. With the increase of Ma number, the larger the angle of attack, the larger the increase of the peak value of the heat flow at such angle of attack. For example, when Ma = 15, the heat flow peak value at α = 25 ° is equivalent to that at α = 0 °, and when Ma = 20, the heat flow peak value at α = 25 ° is higher than that at α = 0 °. When Ma = 20, the heat flow peak value at α = 30 ° is close to twice the peak value at α = 0 °. Therefore, if the flight attitude is at large angle of attack when the vehicle flies at high Ma, the peak value of bottom heat flow at such angle of attack should be considered.

With the increase of Ma number, the bottom heat flow value at each angle of attack increases. From Ma = 5 to Ma = 20, the peak value of heat flow increases by 9.3 times at α = 0 ° and 31.1 times at α=30°. For the higher Ma number, the location and magnitude of the peak value of the heat flow change with the angle of attack at a smaller angle of attack. As shown in Figure 3 (d), the peak value of heat flow from α = 0 ° to α = 5 ° decreases to about 1/3 at α = 0 °, and the location varies from the center line r/R = 0 to r/R = 0.5. With the increase of the angle of attack, the location of the heat flow peak value varies little.

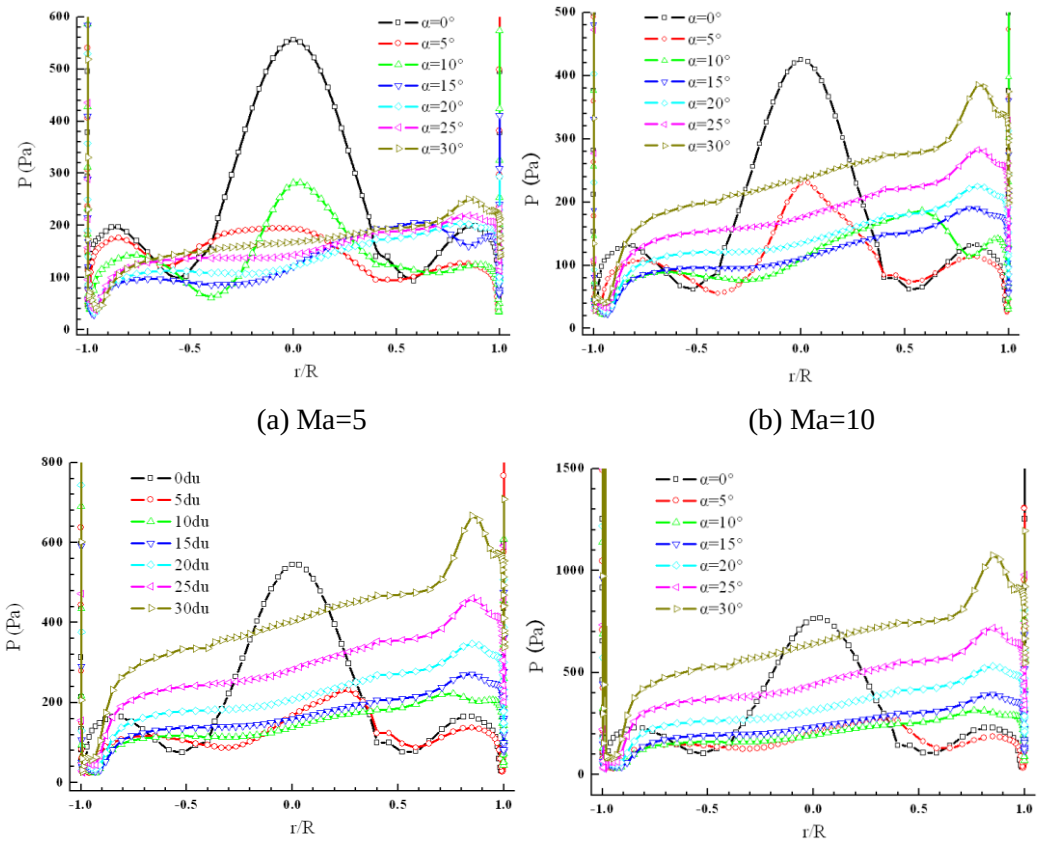

(a) Ma=5 (b) Ma=10

(c) Ma=15 (d) Ma=20

Figure 4. Pressure of center line with the effect of angle of attack.

The pressure distribution on the bottom center line is shown in Figure 4. The trend of the pressure and heat flow with the change of the angle of attack and Ma number is similar to the heat flow. When α = 0 °, the peak value of pressure appears at the center of the bottom. When the angle of attack occurs, the pressure on the leeward side is reduced and the flow line on the conical surface flows along the cone to the leeward side. At the same time, the bottom stagnation point moves toward the leeward side. At high Ma, the pressure distribution along the centerline is more evenly distributed than the heat flow distribution.

3.3. The rule of the bottom flow field with the change of angle of attack and Ma number

The Ma distribution of the bottom flow field of the flight vehicle at Ma = 20 is shown in Figure 5, and the topology of the wake flow field at other Ma numbers is similar to that at Ma = 20. The wake flow field at the angle of attack α = 0 ° is shown in Figure 5. It can be seen that there is a very large Prandtle-Meyer dilatational wave region in the shoulder region of the flow field at the bottom of the flight vehicle and a large recirculation zone at the bottom of the flight vehicle. The downstream flow field produces the recompression shock wave, and the reattachment point position is in the vicinity of the downstream L / R ≈ 1.49. As the Ma number increases from 5 to 20, the position decreases to near L / R ≈ 1.26. At the calculated angle of attack, no separation occurs on the leeward side of the flight vehicle. With the increase of the angle of attack, the shear effect of the bottom flow field is enhanced; the area of the bottom flow field is reduced; and the recirculation zone and the bottom stagnation point move toward the leeward side.

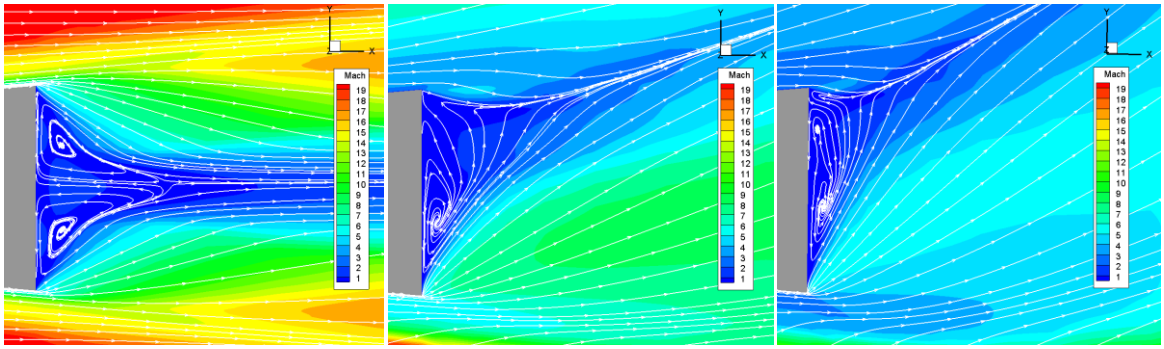

(a) α=0 ° (b) α=15 ° (c) α=30 °

Figure 5. Contour of Ma with the effect of angle of attack, Ma=20.

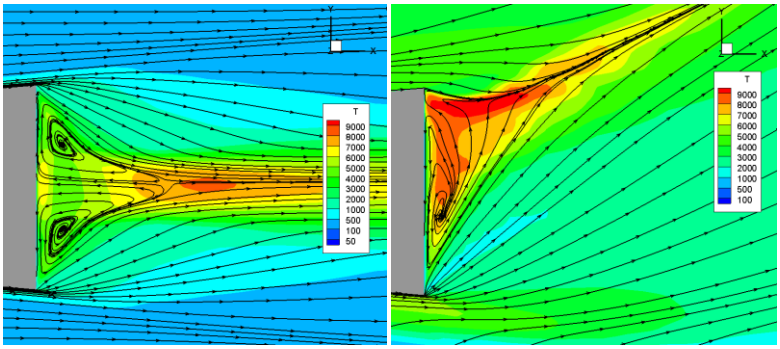

(a) α=0 ° (b) α=25 °

Figure 6. Contour of temperature with the effect of angle of attack, Ma=20.

The temperature distribution of the bottom flow field at Ma = 20 is shown in Figure 6. It can be seen that the temperature near the stationary point of the recirculation zone in the wake flow field is very high at α = 0°. With the increase of the angle of attack, the recirculation zone moves toward the bottom leeward direction and is closer to the wall, thus the bottom heat flow increases.

The distribution of the bottom heat flow with the change of the angle of attack at Ma = 20 is shown in Figure 7. It can be seen that the maximum value of the heat flow at α = 0 ° appears at the center of the bottom. As the angle of attack increases, the peak value of the heat flow moves toward the leeward side. However, at the same time, we can see that apart from the heat flow and pressure peak areas near the leeward side on the center line, there are two relatively concentrated areas of heat flow and pressure near the center line of the leeward side. When the angle of attack occurs, the pressure on the leeward side of the flight vehicle cone is reduced and the flow line on the conical surface flows along the cone to the leeward side, which changes the shape of the recirculation zone.

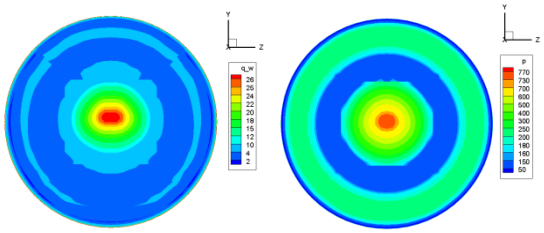

(1) α=0 °

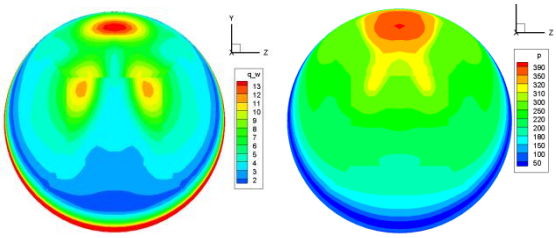

(2) α＝15 °

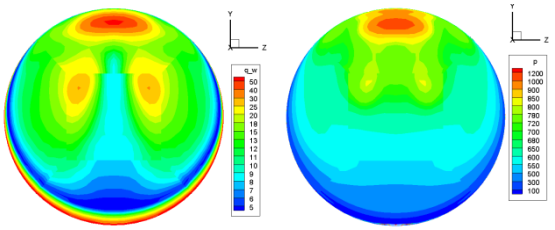

(3) α＝30 °

(a) Heat flux (b) Pressure

Figure 7. Contour of heat flux and pressure with the effect of angle of attack, Ma=20.

4. Conclusions

In this paper, the effects of the angle of attack and Ma number on the aerodynamic heating of the bottom flow field of a hypersonic flight vehicle are studied. The result shows:

(1) As the angle of attack increases, the peak value of the heat flow at the bottom of the flight vehicle moves toward the leeward side, and the peak value of heat flow decreases first and then increases.

(2) With the increase of Ma number, the bottom heat flow value at each angle of attack increases. The greater the Ma number, the more obvious the peak value of bottom heat flow that changes with the angle of attack.

(3) With the increase of the angle of attack, the shear effect of the bottom flow field is enhanced; the recirculation zone of the bottom flow field is reduced; and the recirculation zone and the bottom stagnation point move toward the leeward side.

Reference:

[1] J.Parker Lamb, William L. Oberkampf. Review and development of base pressure and base heating correlations in supersonic flow[J]. Journal of Spacecraft and Rockets, Vol.32, No.1, 1995:8-23.

[2] Datta V. Gaitonde. Mean flowfield structure of a supersonic three-dimensional base flow[J]. Journal of Aircraft, Vol. 47(2):368-382, 2010.

[3] Krishnendu Sinha, Effect of Reynolds Number on Detached Eddy Simulation of Hypersonic Base Flow[R], AIAA-2007-1457, 2007.

[4] Michael Barnhardt, Graham V. Candler. Detached eddy simulation of hypersonic base flows during atmospheric entry[R]. AIAA-2006-3575, 2006.

[5] Dillon, J. L, Carter, H. S. Analysis of Base Pressure and Base Heating on a 5º Half-Angle Cone in Free Flight Near Mach 20 (Reentry F), NASA-TM X-2468, 1972.

[6] T.C. Lin, L,K. Sproul. Hypersonic reentry vehicle wake flow fields at angle of attack[R]. AIAA-2006-582, 2006.